King's Research Portal

Document Version
Peer reviewed version

[Link to publication record in King's Research Portal](#)

3D full-colour image projection based on reflective metasurfaces under incoherent illumination

Diane J. Roth,*,†,‖ Mingke Jin,‡,‖ Alexander E. Minovich,*,†,¶,‖ Song Liu,§ Guixin Li,‡,§ and Anatoly V. Zayats†

†Department of Physics and London Centre for Nanotechnology, King's College London, Strand, London WC2R 2LS, UK

‡Department of Materials Science and Engineering, Southern University of Science and Technology, Shenzhen 518055, China

¶Current address:

Institute of Applied Physics, Abbe Center of Photonics, Friedrich Schiller University Jena, 07745 Jena, Germany

§Shenzhen Institute for Quantum Science and Engineering, Southern University of Science and Technology, Shenzhen 518055, China

‖Author contributions:

These authors contributed equally to this work

E-mail: diane.roth@kcl.ac.uk; min124@physics.anu.edu.au

Abstract

Metasurfaces provide an efficient approach to control light wavefronts and have emerged at the forefront of digital holography. Nevertheless, full-colour image projection remains challenging. Using a combination of specular and diffuse reflections from

a metasurface, in analogy to the normal mapping technique, we designed a reflective metasurface performing in the whole visible spectral range to demonstrate 2D images with shading effects of 3D objects. The non-interleaved metasurface is based on aluminum nanostructures with high and relatively uniform efficiency across the visible spectrum. It operates under incoherent illumination and does not require polarising optics to observe images. The integration of the metasurface behind pre-existing transparent colour images is also demonstrated for introduction of 3D effects. Emulating colour 3D images with flat metasurfaces can be useful for security applications and decorative purposes. The design of broadband metasurface diffusers is also interesting for flat optical diffusing elements with engineered properties and display technology.

Keywords

Metasurfaces, 3D effects, holography, optical diffusers, normal mapping

Dielectric and plasmonic metasurfaces provide excellent control over the shaping of optical wavefronts via the manipulation of polarisation, phase and amplitude of light.[1] Taking advantage of their subwavelength thicknesses, metasurfaces have shown to be a very promising technology in a variety of applications including beam steering and focusing, polarisation and angular momentum control, enhancement of nonlinear effects, as well as holographic imaging.[1–3] Metasurface-based holography has recently attracted attention owing to the exquisite control and flexibility offered by metasurfaces compared to conventional holography techniques,[4] which results in subwavelength pixel resolution, higher diffraction efficiency, and potential full-color performances. However, the design of highly efficient metasurfaces operating across the whole visible spectral range still represents a significant challenge. Typical approaches for color holography are based on either spatial multiplexing of different wavelength-dependent elements into large unit cells (interleaved designs)[5,6] or wavelength-dependent off-axis illumination.[7,8] These methods have, therefore, significant

limitations. In the case of interleaved designs, the broadband spectral response of the meta-surface is achieved by the combination of elements of different sizes designed for each (red, green, blue) wavelength,[6] resulting in large combined pixels degrading the image quality, as well as cross-talk between the higher-order diffraction patterns. Cross-talk issues have been solved by the use of metasurfaces with identical meta-elements but an off-axis illumination, therefore necessitating different angles of incidence for different wavelengths.

Here, we demonstrate the design, fabrication and characterisation of a broadband reflective metasurface structure operating throughout the whole visible spectral range, including the main color wavelengths red, green, and blue (RGB). Unlike the typical techniques to achieve broadband performances, the metasurface presented in this work is based on a simple, non-interleaved design of identical meta-atoms, and implements the notion of diffuse reflection and the concept of normal mapping to control its scattering properties. To illustrate the performance of the metasurface design, we demonstrated a 2D image of a cube with lighting and shading effects, which change according to the illumination angle, emulating the behaviour of a real 3D cube (Figure 1a). We further demonstrated that the integration of the metasurface behind a transparent film with 2D colour images introduces 3D effects to pre-existing 2D images. These operating modalities can be useful for security applications, as well as artistic and decorative purposes on flat surfaces and display technology. The approach may be of interest for the design of broadband flat metasurface-based diffusers, as an alternative to current implementations based on microlens arrays.

When a metasurface imposes a linear phase gradient on the wavefront, the angle of reflection from the metasurface is defined by the generalised Snell's law.[9] Therefore, the angle of incidence and the angle of reflection can in general be different (Figure 1b). In this case, the reflection is called specular, which means that the image formed by the metasurface is only visible for certain incident angles from a fixed observation point. However, when a linear phase gradient is combined with a parabolic phase pattern to introduce diffuse reflection, the variation of the angle of incidence leads to a smooth and progressive brightness change for
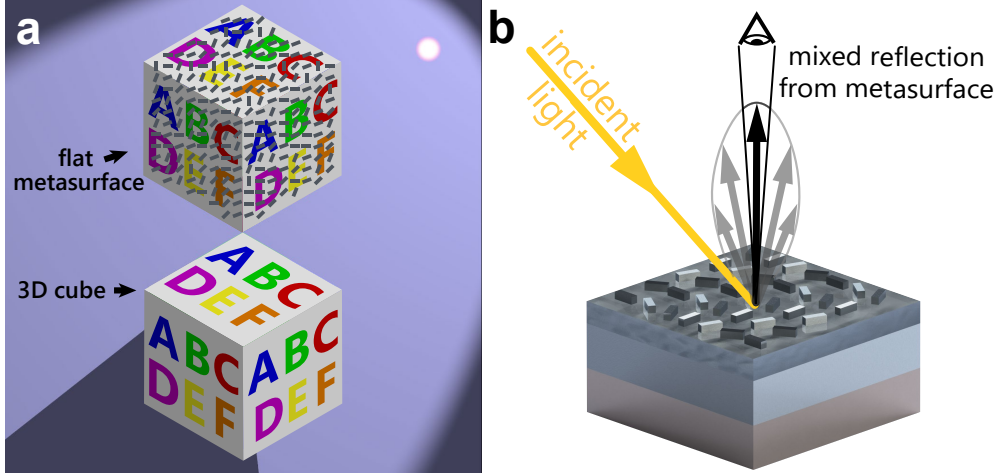
3

Figure 1: (a) Schematic representation of a flat metasurface (top) used to mimic the shading and lighting effects of a white 3D cube and a real 3D cube (bottom). The light source location is marked by a small bright ball. (b) Schematic illustration of mixed specular-diffuse reflection at the normal direction from a metasurface (black-grey) towards an observer. The mirror reflected incident light is directed away from the observer (not shown).

an observer (Figure 1b). Using this mixed specular-diffuse reflection method, it is possible to mimic the normal mapping technique typically used in computer graphics[10] and reproduce shading effects. In other words, the brightness of a flat metasurface changes in response to the variation of the position of a light source, thus imitating the perception of a real 3D object.

In order to imitate a 3D cube, the phase pattern, imposed onto the reflected wave by the metasurface, is the combination of two parts. The first part is a linear phase gradient, defined separately for each cube face. This linear phase gradient determines the direction of the surface normal, if we follow the normal mapping technique analogy.[10] It is designed to reflect towards the observer the light incident in the direction normal to the cube face. The second part is a parabolic phase distribution, which provides the diffuse scattering effect and essentially mimics the effect of a microlens, usually used in macroscopic optics to achieve diffuse scattering. The combination of these two phase distributions results in an off-centered parabolic phase distribution (Figure 2a). This phase pattern is then arranged in 2D square patches (size $7\,\mu$m), which are periodically repeated over the face of the cube (Figure 2b-c).

To avoid discrete diffraction orders due to their periodic arrangement, each square patch has a random constant phase offset, following the approach for the microlens diffusers.[11,12] The value of the radius of curvature r of the diffuser, providing the parabolic phase distribution, is also chosen randomly in the range 10–$15\,\mu$m for each square patch. This helps to further suppress the unwanted diffraction orders. The tight square filling scheme for the phase patches helps to overcome the image graininess problem (see Supporting Information for the details of the design algorithm).
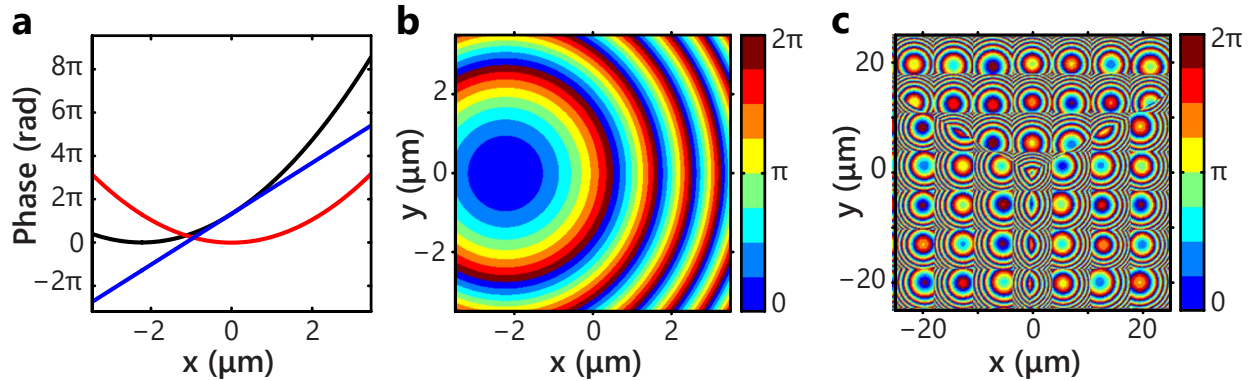

Figure 2: (a) Phase distribution within a microscopic square metasurface patch. A parabolic phase function (red curve) is combined with a linear gradient (blue curve) and results in the phase pattern required to achieve combined specular-diffuse scattering (black curve). (b) Phase distribution as in (a), represented in 2D and discretized in 8 levels from 0 to 2π. (c) Phase pattern of the metasurface representing a cube, consisting of periodically arranged multiple square patches as in (b), randomised to avoid unwanted diffraction orders due to periodicity (see Supporting Information for the design procedure). The individual patch size is $D = 7\,\mu$m and the radius of curvature of the diffuser r is randomly distributed in the range $r = 10$–$15\,\mu$m.

The designed phase pattern was implemented using a Pancharatnam-Berry geometric phase method based on a reflective metasurface[13] and circularly polarised incident light. The phase modulation is controlled by the orientation of subwavelength aluminum nanorods located above an aluminum ground layer (Figure 3a). The nanorods are separated from the ground layer by a magnesium fluoride (MgF_2) dielectric layer. To protect the aluminum metasurface from oxidation, the structure is also covered by a thin layer of the same dielectric, thus completely surrounding the nanorods. With such a design, the helicity of the

incident circularly polarised light is preserved, so that specular-diffuse reflected light modulated by the metasurface has the same helicity as the incident light. This is different from transmissive metasurfaces for which the helicities of the incident and transmitted light are opposite. In order to achieve a broadband response across the visible spectral range, the two plasmonic resonances, corresponding to the electric field polarized along and perpendicular to the nanorod axis, should be positioned on the opposite sides of the operating spectral range[14] (see Supporting Information for the details). Aluminum was chosen because it supports plasmonic resonances at higher frequencies than other materials, such as gold or silver, therefore extending the operating range of the structure to the whole visible spectrum, particularly the blue spectral range.[5]

To find the best geometric parameters for the metasurface elements, numerical simulations using the CST Microwave Studio Finite-Difference Frequency-Domain (FDFD) solver were performed. The main challenge in the design of the metasurface unit cell was to achieve a good efficiency at high frequency (blue spectral range). In this range, surface-plasmon polaritons (SPPs) are excited at the metal-dielectric interface due to the periodicity of the structure (see Supporting Information for more details). This results in an unwanted drop in reflection, compromising the broadband efficiency of the structure. In order to move the SPP resonance to higher frequencies, the use of aluminum was preferred as a ground layer material over silver, also suitable in the blue-wavelength range. Despite its lower reflection compared to silver, aluminum provides a better positioning of the SPP resonance, which is crucial for the realisation of the broadband response. As a result of the optimisation process, the period of the structure was chosen as $P_x = P_y = 190$ nm, in order to allow SPP excitation only for angles of incidence larger than $\theta_i = 30°$ (Figure 3b), so that the reflection and, therefore, the efficiency of the metasurface remain high for incident angles smaller than $\theta_i = 30°$. Further reduction of the period could not be made because of the length of the nanorods, as the smaller dimensions would affect the performance of the structure in the red spectral region. This reduced size of the unit cell, however, results in some small cross-talk

6

between the neighbouring nanorods, which can be noticed for different nanorod rotation angles φ_a (see Supporting Information for more details). The optimised structure shows a reflectance larger than 65% for incident angles up to $\theta_i = 30°$ in a broad spectral range from 460 nm to 610 nm (Figure 3b).
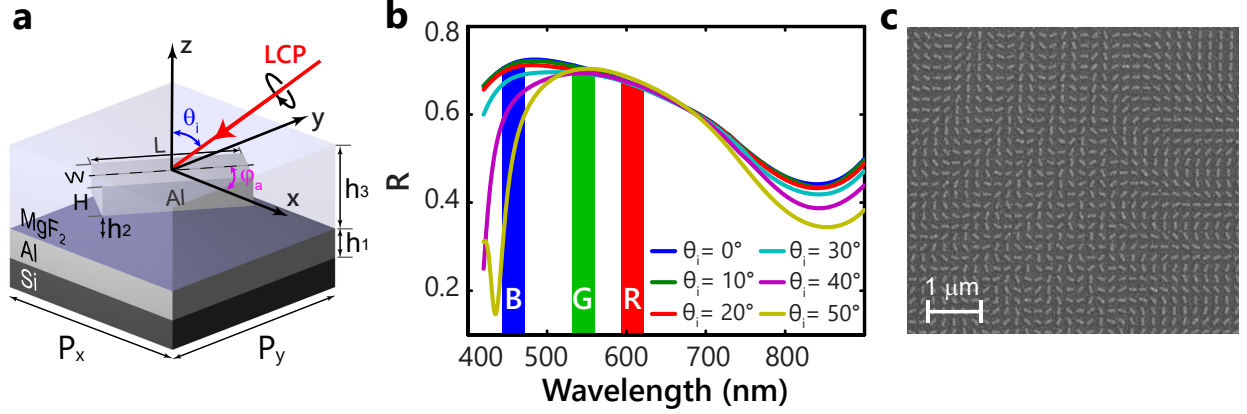

Figure 3: (a) Schematic representation of a metasurface unit cell ($h_1 = 100$ nm is the aluminum film thickness, $h_2 = 30$ nm is the MgF$_2$ spacer thickness, $h_3 = 100$ nm is the MgF$_2$ protective layer thickness, $P_x = P_y = 190$ nm are the unit cell sizes in $x-$ and $y-$directions, respectively, $L = 150$ nm, $W = 60$ nm, and $H = 30$ nm are the aluminum nanorod length, width, and height, respectively. Illumination configuration is also shown with φ_a being the angle of rotation of the nanorod with respect to the x-axis and θ_i being the angle of incidence (in the xz plane). (b) Numerically simulated reflectance spectra (LCP) for the nanorods with $\varphi_a = 0°$ and different angles of incidence θ_i. Color bars mark the maxima of the camera sensitivity in each RGB channel: 610 nm for R, 540 nm for G, 460 nm for B. (c) SEM image of the fabricated metasurface.

The designed metasurface was fabricated using electron beam lithography (EBL) (see Supporting Information for the details). The phase pattern required to imitate a 3D cube is encoded in 8 steps via the rotation of the nanorods, which induce the phase modulation $\Phi = 2\varphi_a$ for the reflected wave (Figure 3c). For the image projection, the metasurface pattern is illuminated by a weakly focused, incoherent white light source (tungsten-halogen lamp) at a varying angle of incidence θ_i. The structure performs under incoherent light because a coherence length of the source of the order of the size of a single square phase patch ($7\,\mu$m in our case) is sufficient for the operation of the metasurface pattern, according to the Van Cittert-Zernike theorem.[15] A broadband polarizer and a quarter-wave plate are used

to produce the left circular polarization (LCP) of the incident beam. Specular and diffuse light with the same helicity as the incident light (LCP) is generated due to the geometric phase modulation from the metasurface in the direction normal to the metasurface, at which observations are made. This LCP light is collected by a lens and imaged onto a colour CMOS camera (see Supporting Information for the details on the experimental setup). A small part of the incident LCP light, which is not affected by the metasurface, is mirror reflected with an opposite helicity (RCP), and is not observed in the direction normal to the surface. Therefore, no additional polarising optics (analyser) is needed after the light is reflected by the metasurface, as only LCP light is directed along the normal to the surface. For image observation, the white color balance of the camera was first set using the image of a white paper sheet and the gains of the three RGB color channels were adjusted to get equal signal in each of them. The full-color image has a slight blue-green hue (Figure 4a) because the implemented phase pattern was optimized for a central wavelength of 532 nm, in the middle of the operational range (as described in Supporting Information). All three RGB channels contain almost equal signal levels.

Several projections of the cube were then recorded for different angles of illuminations of the metasurface from $\theta_i = 20°$ to $\theta_i = 70°$ (Figure 4b). The metasurface performs similarly to a 3D object: the faces turned towards the light source become dimmer for higher angles of incidence. Up to an incident angle of approximately $\theta_i = 30°$, the colouring of the projected image remains practically the same, however, its brightness decreases with the incident angle, as the diffraction efficiency decreases for the main RGB wavelengths (Figure S4c). For large incident angles, the pattern colour changes from blue-green to red, due to the non-uniform change of the efficiency of the metasurface with the increase of the angle of incidence (Figure 3b). These observations are in agreement with the angular distribution of the reflectance for different wavelengths (Figure S4b-c).

In order to demonstrate the potential of the designed metasurface for the introduction of 3D perception of pre-existing 2D colour images, the metasurface was combined with

transparent photographic film slides (reversal film) with printed colour images. A digital color checker pattern (Figure 4c) was printed on a 36 x 24 mm slide using a resolution of 8192 x 5462 pixels. This pattern displays colour images when observed in transmission, but no 3D effects (Figure 4e). When the slide is carefully positioned on top of the metasurface to match the color checker pattern and the metasurface (Figure 4d), the 3D shadowing effects are observed for each individual RGB parts as well as a white part of the pattern (Figure 4f). The metasurface performance remains globally the same: the faces closer to the light source become brighter. The slightly less pronounced 3D effects are the result of the lower contrast of the image, due to the increased scattering of the light from the film in the darker regions (opposite to the light source). In this demonstration, the metasurface acts as a back diffuser, similar to LCD display designs.

The projected images were also observed for a fixed angle of illumination θ_i but different angles of rotation of the metasurface γ_s (Figure 5). The faces of the cube become brighter when turned towards the light source, and *vice versa*, as a real 3D object behavior. While these observations were performed using the experimental set-up in Figure S5a, very similar quality of the 3D image can be obtained using standard 3D cinema glasses (circular film polarizers) instead of the the research-grade broadband polarizer and quarter waveplate in the illumination path, emphasising the practical potential of the design (Figure S6).

In summary, we have demonstrated a full-colour visible-band metasurface that generates 3D images by emulating shading effects upon changes of the illumination conditions. Unlike typical metasurface-based holography techniques, this method does not rely on interleaved nanostructures for wavelength multiplexing or wavelength-dependent off-axis illumination to achieve full-color imaging. Using a simple but carefully optimised metasurface design, the structure shows broadband performance and its operating range includes the main visible colors: red, green, and blue. The metasurface operates under incoherent illumination with an incandescent light bulb and is tolerant to the quality of the polarisation of the illuminating light, so that an illumination through inexpensive 3D cinema glasses can be
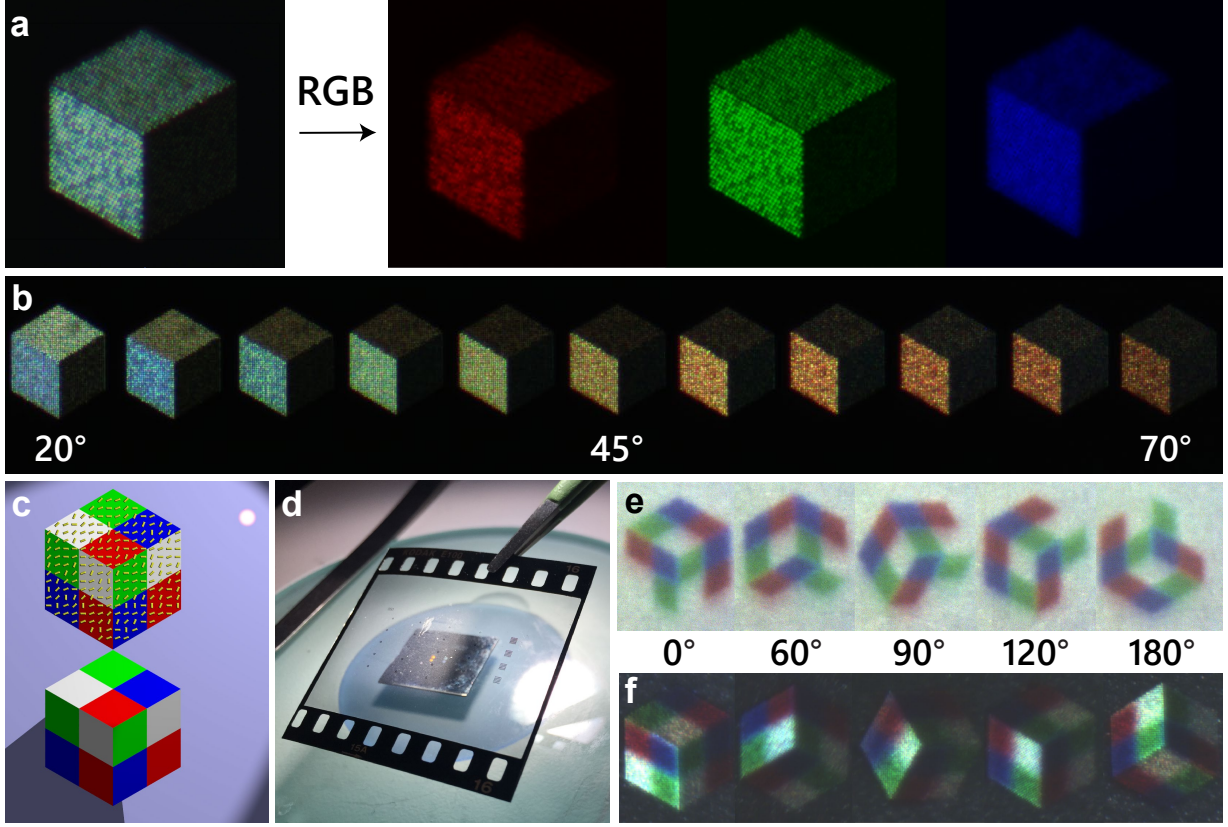
Figure 4: Color image generated by the metasurface observed in the direction normal to the sample, while illuminated by incoherent white light at the incident angle $\theta_i = 30°$, together with the images in separate red, green, and blue colour channels. (b) The dependence of the colouring and brightness of the image on the angle of illumination ranging from $\theta_i = 20°$ to $\theta_i = 70°$ with a step of 5° (see Figure 3a for the definition of the angles). (c) Schematic representation of the 2D digital color checker pattern used for visualisation. (d) The transparent photographic film slide with printed color checker pattern placed on top of the metasurface. (e-f) The observed images (e) without and (f) with the metasurface behind the transparent slide with a colour checker pattern. Images recorded at different angles of rotation γ_s of the metasurface illuminated at an angle of incidence $\theta_i = 30°$ from the left side.
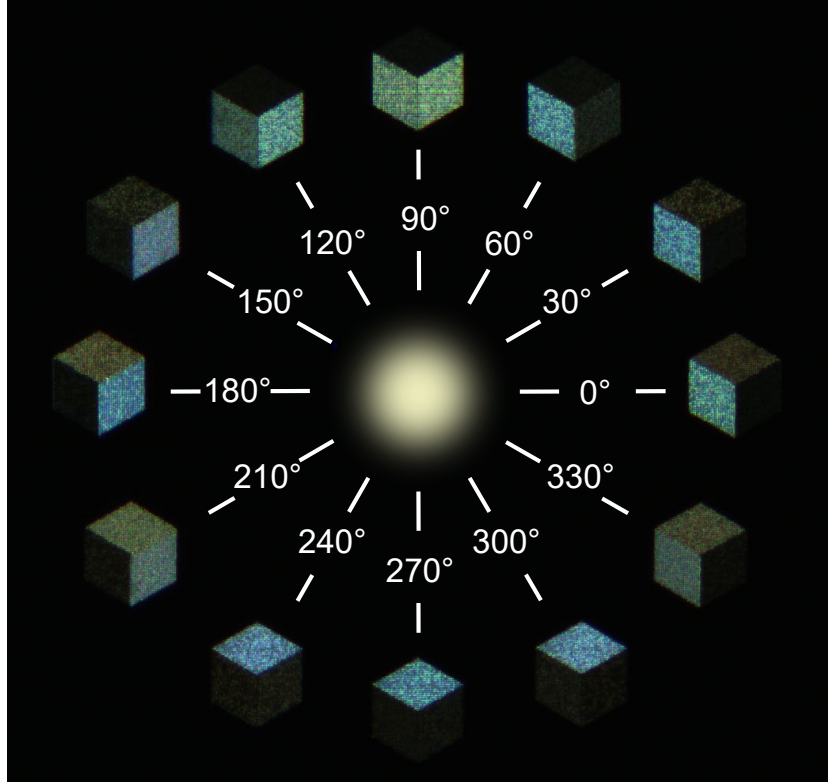
Figure 5: The cube images observed for different angles of rotation γ_s of the metasurface. The angle of incidence is fixed to $\theta_i = 30°$. The metasurface is illuminated with white incoherent light.

used and integrated directly onto a metasurface. No polarisation optics is required in the observation path. The metasurface can also be used as a back reflector to introduce 3D perception of pre-existing transparent 2D colour images. The visual 3D effects relying on color metasurface-based image generation can be used for security applications, where different methods, such as rainbow holograms, are used in hologram stickers for protection against counterfeiting. Dynamically controlled metasurface structures can also be achieved for the realization of 3D motion pictures.[16] More generally, the interesting properties of the diffuse scattering from planar metasurfaces with nanoscale design can find applications in multiple domains, where diffuse materials or conventional microlens diffusers are typically used, such as in display technology, metrology, as well as in the design of optical systems requiring off-axis geometries and bespoke scattering properties. The phase modulation properties of the metasurface can also be useful for the development of novel optical elements, where surface profiling is not required for beam shaping such as, for instance, in GRIN lenses technology.

Acknowledgement

Supporting Information Available

The following files are available free of charge.

Supplementary Text, Figures S1 to S6: Metasurface phase pattern design, Simulated reflectance spectra, Angular spectrum of reflection, Sample fabrication, Optical set-up, Experimental reflection spectra, Observation under illumination through a circular polarizer for 3D movie viewing.

References

(1) Yu, N.; Capasso, F. Flat optics with designer metasurfaces. *Nature Mat.* **2014**, *13*, 139–150.

(2) Kildishev, A. V.; Boltasseva, A.; Shalaev, V. M. Planar photonics with metasurfaces. *Science* **2013**, *339*, 1232009.

(3) Minovich, A. E.; Miroshnichenko, A. E.; Bykov, A. Y.; Murzina, T. V.; Neshev, D. N.; Kivshar, Y. S. Functional and nonlinear optical metasurfaces. *Laser & Photonics Reviews* **2015**, *9*, 195–213.

(4) Deng, Z.-L.; Li, G. Metasurface optical holography. *Materials Today Physics* **2017**, *3*, 16–32.

(5) Huang, Y.-W.; Chen, W. T.; Tsai, W.-Y.; Wu, P. C.; Wang, C.-M.; Sun, G.; Tsai, D. P. Aluminum plasmonic multicolor meta-hologram. *Nano Letters* **2015**, *15*, 3122–3127.

(6) Wang, B.; Dong, F.; Li, Q.-T.; Yang, D.; Sun, C.; Chen, J.; Song, Z.; Xu, L.; Chu, W.; Xiao, Y.-F.; Gong, Q.; Li, Y. Visible-frequency dielectric metasurfaces for multiwavelength achromatic and highly dispersive holograms. *Nano letters* **2016**, *16*, 5235–5240.

(7) Wan, W.; Gao, J.; Yang, X. Full-color plasmonic metasurface holograms. *ACS nano* **2016**, *10*, 10671–10680.

(8) Li, X.; Chen, L.; Li, Y.; Zhang, X.; Pu, M.; Zhao, Z.; Ma, X.; Wang, Y.; Hong, M.; Luo, X. Multicolor 3D meta-holography by broadband plasmonic modulation. *Science advances* **2016**, *2*, e1601102.

(9) Yu, N.; Genevet, P.; Kats, M. A.; Aieta, F.; Tetienne, J.-P.; Capasso, F.; Gaburro, Z. Light propagation with phase discontinuities: generalized laws of reflection and refraction. *Science* **2011**, *334*, 333–337.

(10) Ganovelli, F.; Corsini, M.; Pattanaik, S.; Di Benedetto, M. *Introduction to Computer Graphics: A Practical Learning Approach*; CRC Press, 2015; p 422.

(11) Morris, G. M.; Sales, T. R. M. Structured screens for controlled spread of light. US Patent No 7033736, 2001.

(12) Sales, T. R. M.; Schertler, D. J.; Chakmakjian, S. Deterministic microlens diffuser for Lambertian scatter. *Proc. SPIE* **2006**, *6290*, 629005–10.

(13) Zheng, G.; Mühlenbernd, H.; Kenney, M.; Li, G.; Zentgraf, T.; Zhang, S. Metasurface holograms reaching 80% efficiency. *Nature Nanotechnology* **2015**, *10*, 308–312.

(14) Minovich, A. E.; Zayats, A. V. Geometric-Phase Metasurfaces Based on Anisotropic Reflection: Generalized Design Rules. *ACS Photonics* **2018**, *5*, 1755–1761.

(15) Born, M.; Wolf, E. *Principles of optics*; Cambridge University Press, Cambridge, 2005; p 572.

(16) Bar-David, J.; Stern, L.; Levy, U. Dynamic Control over the Optical Transmission of Nanoscale Dielectric Metasurface by Alkali Vapors. *Nano Letters* **2017**, *17*, 1127–1131.

Graphical TOC Entry